

On the Scaling Law for Broadband Shock Noise Intensity in Supersonic Jets

Max Kandula¹

ASRC Aerospace, NASA Kennedy Space Center, Florida 32899, USA

A theoretical model for the scaling of broadband shock noise intensity in supersonic jets was formulated on the basis of linear shock-shear wave interaction. An hypothesis has been postulated that the peak angle of incidence (closer to the critical angle) for the shear wave primarily governs the generation of sound in the interaction process rather than the noise generation contribution from off-peak incident angles. The proposed theory satisfactorily explains the well-known scaling law for the broadband shock-associated noise in supersonic jets.

Nomenclature

c	= sound speed, $\sqrt{\gamma p / \rho}$
c^*	= critical sound speed
c_p	= specific heat at constant pressure
d_j	= nozzle diameter
d_e	= effective jet diameter
f	= frequency
I	= acoustic intensity
\mathbf{k}	= wave vector
k	= wave number; also turbulent kinetic energy
L	= shock-cell spacing
M_c	= convective Mach number, u_c / c_∞
M_d	= design Mach number
M_j	= fully expanded jet Mach number
$P(\theta)$	= transfer function for sound wave generation
p	= pressure
p_{ref}	= reference sound pressure, $2 \times 10^{-5} \text{ N/m}^2$
R	= gas constant
Re_j	= jet exit Reynolds number, $\rho_{je} u_{je} d_j / \mu_{je}$
SPL	= sound pressure level
T	= temperature
u_c	= convective velocity
u	= velocity in the streamwise direction
x	= axial distance from the nozzle exit plane

¹ Mailstop ASRC-5211, Associate Fellow AIAA.

Greek Symbols

β	=	$(M_j^2 - 1)^{1/2}$
γ	=	isentropic exponent
μ	=	dynamic viscosity
ρ	=	density
θ	=	observation angle relative to the downstream jet axis

Subscripts

0	=	ambient fluid
<i>cr</i>	=	critical
<i>e</i>	=	nozzle exit
<i>j</i>	=	jet
ref	=	reference
<i>t</i>	=	stagnation (total)

I. INTRODUCTION

Noise from subsonic jets is mainly due to turbulent mixing, according to the theoretical model of Sir James Lighthill.^{1,2} The turbulent mixing noise is essentially broadband. In perfectly expanded supersonic jets (nozzle exit plane pressure equals the ambient pressure), the large-scale mixing noise manifests itself primarily as Mach wave radiation (Ffowcs Williams³) caused by the supersonic convection of turbulent eddies with respect to the ambient fluid. In imperfectly expanded supersonic jets (nozzle exit pressure different from the ambient pressure) typical of jet and rocket exhausts at off-design conditions, additional noise is generated (Fig. 1, see Ref. 4) in the form of broadband shock-associated noise (BBSN) emanating from shock-turbulence interaction (Harper-Bourne and Fisher⁵) and screech tones (Powell^{6,7}) with the tonal (screech) amplitude shown to be occasioned by shock-acoustic wave interaction⁸.

In imperfectly expanded supersonic jets, the rapid variation in the pressure across the nozzle exit is accompanied by a system of steady compression (oblique shock) and expansion waves (Fig. 2). The structure of these shock cells was investigated by Emden⁹, Prandtl¹⁰, Lord Rayleigh¹¹, Pack¹², and others. The broadband shock noise is of relatively high intensity, and may form a significant component of the overall jet noise, depending on the flow conditions. A fundamental understanding of the mechanism by which turbulence interacts with a shock wave is thus requisite in the analysis of the complex phenomena of shock noise generation.

Lighthill¹³ and Ribner^{14,15} originally suggested that the scattering of eddies by shocks could be a strong source of supersonic jet noise. The importance of source coherence, however, has not been recognized, so that only incoherent and randomly scattered sound waves had been predicted without the peak frequency and directivity relationships. It was Harper-Bourne and Fisher⁵ who first identified the detailed characteristics of BBSN with the aid of measurements from conical (convergent) nozzles, and indicated the importance of source coherence. The characteristics of shock noise were also reviewed and discussed in Fisher et al.¹⁶ Howe and Ffowcs Williams¹⁷ also considered that the primary source of broadband shock-associated noise is a consequence of the interaction between large scale structures (turbulence) and the shock structure.

Computing shock noise intensity in supersonic jets from first principles (on the basis of shock-turbulence interaction) is very difficult. The nature of the relevant noise sources is not well understood (Krothapalli¹⁸). This situation is exemplified by the fact that the theories of both Lighthill¹³ and of Ribner^{19,20} produce shock noise intensity scaling considerably different from that indicated by the measurements.

It is the purpose of this work to investigate the scaling of shock noise intensity from fundamental considerations. It is demonstrated here that the scattering of turbulence by the leading shock wave is related to the measured shock noise intensity scaling. Flight effects are excluded from consideration here. Also screech effects are not relevant to this investigation.

II MEASUREMENTS AND CHARACTERISTICS OF BROADBAND SHOCK NOISE

A. Intensity of Shock Noise

Harper-Bourne and Fisher⁵ were the first to identify significant features of shock-noise in considerable detail based on their static jet measurements from conical nozzles. The intensity of BBSN is shown to be primarily a function of the nozzle (operating) pressure ratio (NPR = p_t / p_0). For a given radiation direction, the measured overall sound intensity I has been observed to scale as (Fig. 3)

$$I \propto \beta^4 \quad (1a)$$

where

$$\beta = (M_j^2 - 1)^{1/2} \quad (1b)$$

with the isentropic relation between p_t / p_0 and M_j expressed by

$$\frac{p_t}{p_0} = \left(1 + \frac{\gamma - 1}{2} M_j^2\right)^{\gamma/(\gamma - 1)} \quad (1c)$$

In the preceding relations, the quantity M_j represents the fully expanded jet Mach number, and the parameter β^2 characterizes the pressure jump across a normal shock at approach Mach number M_j . Harper-Bourne and Fisher (1973) found that the parameter β correlated BBSN quite well up certain values of β (or NPR), say $0.5 < \beta < 1.2$. At large NPR or β , the data begin to deviate from this law because of the presence of a Mach disc, which significantly alters the shock-cell structure. As the Mach disc forms, the large central portion of subsonic flow formed downstream of the Mach disc considerably reduces the noise generation. The data also reveal that at high β the turbulent mixing noise level is much lower than the underexpanded noise levels. As β decreases, the mixing noise contribution relative to the total noise becomes increasingly significant.

Experiments by Tanna²¹ and of Seiner and Norum²² provided further insight into the characteristics of shock noise. These data include measurements from convergent-divergent (C-D) nozzles, and covered a broad range of jet conditions (NPR and jet temperature ratio). Both Tanna's data²¹, covering $\beta \leq 1$ ($M_j \leq 1.41$, or $p_R / p_0 \leq 3.5$), and the data of Seiner and Norum²² (covering $M_d = 1.5$, and 2 and $M_j = 1$ to 2.37 or $\beta = 0$ to 2.15) suggest trends similar to those indicated by the data of Harper-Bourner and Fisher⁵ to the extent that the overall intensity of shock-associated noise is principally a function of jet pressure ratio, scales as $I \propto \beta^4$, and is independent of jet temperature ratio (efflux temperature) and emission angle.

The data by Krothapalli et al.¹⁸ for broadband shock noise for M_j in the range of 1.24 to 1.66 suggest that the shock noise intensity follows the β^4 dependence for both the stationary ambient ($M_\infty = 0$) and in forward flight ($M_\infty = 0.32$).

B. Spectra and Directivity of Shock Noise

Directivity

Measurements by Tanna²¹ indicate that for all values of T_j/T_0 considered, the directivities from underexpanded jets in the forward arc are essentially flat, indicating that the sound radiated by the presence of shocks in a jet flow is fairly omnidirectional (Fig 4).

Detailed acoustic measurements by Norum and Seiner²³ suggest that the shock noise intensity is not necessarily omnidirectional. The shock noise is fairly directional at lower β values and approaches omnidirectionality only at large values of β . Both the source directivity and the Doppler shift effect may contribute to the far-field directivity (Pao and Seiner²⁴).

According to Krothapalli et al.¹⁸, in cold jets, the shock-associated noise dominates over the turbulent mixing noise except in the aft quadrant. At elevated temperature, the turbulent mixing noise increases, and the shock-associated noise remains unaltered.

Spectra

Fig. 5 displays the spectral characteristics of BBSN according to the data of Tanna²¹, for various angles of observations. The variation of peak frequency (which represents an important characteristic) with the angle of observation is demonstrated. Pao and Seiner²⁴ indicate that the power spectral density (dB/Hz) increases as ω^4 below the peak frequency, and decays as ω^{-2} beyond the peak frequency.

According to the measurements by Krothapalli et al.¹⁸ for broadband shock noise for M_j from 1.24 to 1.66, the broadband spectral peak is dominant in the region of $50 < \theta < 110$ deg. Unlike the screech tone, its peak frequency is a function of the direction of radiation with the lower frequency being near the jet inlet direction ($\theta = 0$).

III MODELS FOR BROADBAND SHOCK NOISE

The semi-empirical model of Harper Bourne and Fisher⁵ forms an important contribution to the theory of BBSN. Alternative models were later proposed by Howe and Ffowcs Williams¹⁷ and Tam and coworkers.²⁵⁻²⁷ Howe and Ffowcs-Williams¹⁷ proposed a theoretical model of the BBSN based on a multiple scattering approach. Tam and coworkers^{26,27} proposed a stochastic model theory for BBSN that showed good agreement with experimental data. These models deal with shock noise intensity, spectra and directionality.

A. Model of Harper-Bourne and Fisher

Harper-Bourne and Fisher⁵ proposed a *semi-empirical* physical model as an extension of Powell's model for screech.^{6,7} Central to their investigation is the intensity scaling provided by Eq. (1a), namely

$$I \propto \beta^4$$

They approximated (idealized) shock-noise sources as a series of point sources located at shock-turbulence interaction locations. The scaling of the spectral peak frequency with shock-cell length, and the correlated nature of shock noise emission from consecutive shock cells were investigated. It was shown (demonstrated) that if the turbulence maintained its coherence as it convected through multiple shock cells, positive (constructive) interference from the sources would result in strong radiation in the upstream direction.

The predicted (and observed) peak frequency was expressed by (see also Fisher et al.¹⁶)

$$f_p = \frac{u_c}{L(1 - M_c \cos \theta)}, \quad (2a)$$

where u_c is the appropriate convection velocity, L the shock-cell spacing, $M_c (= u_c / c_\infty)$ the convective Mach number, and θ the observation angle (direction of noise radiation) relative to the downstream-directed jet axis (jet flow direction). The shock-cell separation L is expressed by

$$L = c_1 d_j \beta \quad (2b)$$

where d_j is the nozzle exit diameter, and c_1 is a constant of proportionality. This relation was theoretically derived by Pack¹². From the measurements, an average value for the constant for the shock-cell array (about eight shock waves) is found to be 1.1. No harmonics are observed in the noise spectra,

A general prediction method for the sound spectra was also developed, requiring input concerning the source spectral density and correlation coefficients, which can be obtained from experiments. The predictions from the model are shown to satisfactorily agree with the data. . .

B. Model of Howe and Ffowcs-Williams

Howe and Ffowcs-Williams¹⁷ proposed a theoretical model for the BBSN, considering the interaction between turbulent velocity fluctuations and the shock-cell system of an imperfectly expanded supersonic jet. Their procedure constitutes a generalization (application) of Lighthill's acoustic analogy¹ of aerodynamic sound to the scattering of a sound wave by turbulence. According to this model, energy is extracted (abstracted) from the ordered nonuniform mean flow of the jet and redistributed into random scattered disturbances. The peak of the noise spectrum is associated with the coherent scattering of sound by the array of shock cells, with additional sound waves produced through multiple scattering forming a wide frequency range of the broadband noise. Isothermal jet is considered, and formulas were derived for the spectra and directivity of BBSN.

With regard to the noise intensity, the model reveals that the predicted sound intensity varies as

$$I \propto \beta^6 \quad (3)$$

This relation is at variance (deviates from) the experimentally observed law (Eq. 1a), showing a fourth power dependence on β . It is pointed out that increasing/decreasing the shear layer width tends to decrease/increase the effective exponent of the predicted power law dependence on β (Howe and Ffowcs Williams¹⁷).

The predicted sound spectrum is characterized by a sequence of peaks produced on account of coherent scattering from successive shock cell. The peak frequency is theoretically found to be consistent with that expressed by Eq. (2), except that the constant is shown to be 1.31. The smaller peaks of the predicted multiple-peaked spectrum are not harmonically related. The directivity of the broadband shock noise is somewhat (essentially) uniform over a wide range of angles in the forward arc.

C. Model of Tam and Coworkers

Tam and Tanna²⁵ presented a shock noise model which considers (weak but coherent) interaction between the downstream propagating instability waves and periodic shock cell system (turbulent eddies regarded as instability waves or large scale turbulent flow structures in the jet mixing layer). Generalizing Harper Bourne and Fisher's β^4 intensity scaling to convergent-divergent nozzles, they proposed a correlation of the form

$$I \propto (M_j^2 - M_d^2)^2 \quad (4)$$

where M_d refers to the nozzle design Mach number. Eq. (4) thus applies to both convergent ($M_d = 1$) and convergent-divergent nozzles. This formula is valid only for weakly imperfectly expanded jets. For convergent nozzles, it reduces to scaling relation of Harper-Bourne and Fisher⁵. Data for a C-D nozzle for $M_d = 1.67$ ($M_j = 1.1$ to 2.0) were also presented, including frequency spectra

A frequency-directivity relation, equivalent to Eq. (2), was derived. The peak frequency is shown to be expressed by

$$f = \frac{u_c}{L_j(1 - M_c \cos \theta)} \quad (5a)$$

where

$$L_j = \frac{2\pi}{\lambda_j} = \pi(M_j^2 - 1)^{1/2} d_e / \mu_1 \quad (5b)$$

with $\mu_1 = 2.40483$, and d_e is the effective jet diameter. The quantity d_e / d_j is a function of M_d, M_j and γ by virtue of conservation of mass flux and isentropic relations (Tam and Tanna²⁵). The above expression for the peak frequency is similar to that of Harper-Bourne and Fisher⁵, as indicated by Eq. (2). With this model, it was suggested that shock-noise should radiate strongly at upstream angles as Mach waves.

Building on the work of Tam and Tanna²⁵, Tam²⁶ formulated a stochastic model theory of the BBSN of axisymmetric supersonic jets by considering the dynamics of weakly nonlinear interaction between linear instability waves (superposition of intrinsic or instability wave modes of the flow describing the spatially and temporally evolving large turbulent structures in the mixing layer) and shock-cell structures (with the standing wave pattern inside the wave guide enclosed by the plume boundary, obtained by multiple-scales expansion). In view of the solution complexity, a final solution was not arrived at; instead a *semi-empirical* (less general) shock noise model, valid for *slightly imperfectly expanded supersonic jets*. Formulas for the nearfield and the farfield spectra were provided by aid of physical reasoning, scaling arguments and data correlation. The results satisfactorily explain in many important aspects of the noise spectra and its directivity pattern. Typically an increase in the spectral peak associated with the BBSN is attributed to the convective amplification of the sources.

The stochastic model theory of BBSN by Tam²⁶ was extended by Tam²⁷ to *moderately imperfectly expanded jets* with the aid of empirical modifications to the amplitude of the waveguide modes of the shock cell. A mathematical theory for the interaction between large turbulent structures and quasi-periodic shock cells is thereby proposed.

IV FUNDAMENTAL STUDIES ON SHOCK-TURBULENCE INTERACTION

A. Theoretical Models

1. Linear Theories

Broadly speaking, the decomposition of a general fluctuation into acoustic, vorticity and entropy waves is well-known (Kovácszay²⁸). In general any plane wave (acoustic, vorticity/shear, or entropy) interacting with a shock undergoes transformation, and at the same time generates the other two waves (Zang et al.²⁹). For example, Fig. 6 shows a schematic of an interaction of a shock wave with an incident vorticity wave. Linear analyses of a single wave (shear/vorticity, acoustic, or entropy) interaction with a shock wave were carried out by Blokhintzev³⁰, Burger³¹, Ribner^{14,15,19,20}, Moore³², McKenzie and Westphal³³.

According to the linear theory, for sufficiently high angles of incidence for the wave ahead of the shock, the incident wave vector \mathbf{k} defined by

$$k = |\mathbf{k}| = 2\pi / \lambda = \omega / c \quad (6)$$

(where λ is the acoustic wavelength, c the sound speed, and ω the circular frequency) has a nonzero imaginary part. Under such circumstances the refracted (or generated) acoustic wave is not an infinite plane wave; instead, it exhibits an exponential decay as it propagates downstream behind the shock. The incidence angle that separates the plane wave acoustic response from the decaying ones is termed the *critical angle*. The critical angle is close to 90 deg. for incident acoustic waves, and roughly 60 deg. for incident vorticity and entropy waves (Zang et al.²⁹). Linear theory predicts that most transmission and generation coefficients are peaked near the critical angle (**evanescent acoustic response?**). From a theoretical point of view, the actual transmission/generation coefficients are independent of the incident wavelength in the linear limit (Zang et al.²⁹).

With regard to broadband shock noise, we are primarily concerned here with shock-turbulence interactions. A turbulent velocity field can be represented as a superposition or spectrum of elementary waves distributed among all orientations and wavelengths in accordance with Fourier's integral theorem. The waves are transverse for weak turbulence because of the constraint of incompressibility (even though convected at high speed). Thus a single wave can be interpreted physically as a plane sinusoidal wave of shearing motion (Batchelor³⁴). According to linear Interaction Analysis (LIA), the vorticity waves incident at angles beyond a critical angle

$$\theta_c = \theta_c(M_1) \quad (7)$$

generate acoustic waves which decay as they propagate downstream. In eq. (7), M_1 refers to Mach number upstream of the shock

Lighthill³ and Ribner^{14,15,19} conducted theoretical analysis on acoustic noise generation by shock wave/turbulence interaction. In **both** Ribner's and Lighthill's theories the turbulence is treated in effect as a *frozen* spatial pattern with neglect of temporal fluctuations.

Ribner's Analysis

Ribner¹³ studied in detail the interaction between a vorticity wave and a shock wave. Ribner^{14,18} extended this analysis to consider a spectrum of incident vorticity waves (in three dimensions) and computed, for an isotropic incident spectrum, detailed statistics of the downstream flowfield with emphasis on the generated noise. The basic building blocks of Ribner's linear theory are oblique plane sinusoidal waves of vorticity (shear waves), see Fig. 6. These represent single spectral (monochromatic) composed of (in 3-D) an instantaneous snapshot of arbitrary flow. The waves are considered to interact independently with the shock, and then the waves are superposed to represent turbulence upstream and downstream of the shock. The detailed statistical formalism was worked out in Ribner¹⁵, and partly summarized by Ribner²⁰.

The mean spectral sound pressure is expressed by^{15,19}

$$\overline{p'^2} = \int_{-\infty}^{\infty} |P(\theta)|^2 [uu] d^3k \quad (8)$$

where $P(\theta)$ is the transfer function for sound wave generation, and $[uu]$ the longitudinal spectral intensity. The initial turbulence is now restricted to be *isotropic*, so that its *longitudinal spectral density* has the general form (Batchelor³⁴)

$$[uu] = k^2 F(k) \cos^2 \theta \quad (9)$$

in spherical coordinates in wave number space, where $F(k)$ is an arbitrary function of k .

For an isotropic turbulence, the acoustic energy flux (per unit area normal to the shock) is finally expressed by

$$I_{ac} = \frac{3p_2^2 \overline{u_2^2}}{2\rho_2 c_2} \int_{\theta_{cr}}^{\pi/2} |P(\theta)|^2 \cos^3 \theta (1 + M_2 \sin \theta^n)(M_2 + \sin \theta^n) d\theta \quad (10a)$$

or

$$\frac{I_{ac}}{I_{turb}} = \frac{3p_2^2}{5\rho_1 \rho_2 c^{*2} c_2 U_1} \int_{\theta_{cr}}^{\pi/2} |P(\theta)|^2 \cos^3 \theta (1 + M_2 \sin \theta^n)(M_2 + \sin \theta^n) d\theta \quad (10b)$$

where the turbulence intensity I_{turb} is defined by

$$I_{turb} = \frac{5}{2} \rho_1 U_1 c^{*2} \langle u_1^2 \rangle \quad (10c)$$

Here θ^n denotes the angle of the refracted shear wave, U the flow speed upstream of the shock, c^* the critical sound speed, and p_1 the ambient pressure. It is necessary to obtain the transfer function $P(\theta)$ and the incident shear wave inclination $\theta^n = f(\theta)$. These quantities are rather cumbersome functions of other functions obtained by Ribner¹⁴ and evaluated and tabulated in Ribner¹⁵ along with the integration limit θ_{cr} . Calculations of the linear theory were performed for an upstream Mach number range of $1 < M_1 < 10$.

The sound pressure level (SPL) is given by²⁰

$$SPL = 20 \log \left(\sqrt{p''} / p_{ref} \right) \quad (11)$$

where p_{ref} is the reference sound pressure ($2 \times 10^{-5} \text{ N/m}^2$). For one percent turbulence, the post shock noise level is predicted to exceed 140 dB for all preshock Mach numbers above 1.05. The velocity components of the post-shock turbulence would be amplified as much as 45 % relative to preshock levels.

Lighthill's Theory

Lighthill¹³ considered the generation of sound due to the interaction of turbulence with very weak shock waves (acoustic-like waves), by aid of his general theory of sound generated aerodynamically (Lighthill^{1,2}). The weak shock is represented by an acoustic step function. In Lighthill's theory the assumptions are more restrictive than in Ribner's analysis in the sense that both the shock and the turbulence are weak. As a result, the rippling motion of the shock as well as the differences in the turbulence intensity across the shock are suppressed. The ratio of freely scattered acoustic energy to the kinetic energy of turbulence traversed by the shock wave is expressed relative to a *frame moving with the fluid*, whereas Ribner's analysis deals with a *frame attached to the shock*.

For a direct comparison, Ribner¹⁹ converted the results of Lighthill¹³ to the shock-fixed reference frame as follows:

$$\frac{I_{ac}}{I_{turb}} = \left(0.2175 - 6\phi + \phi^3 \right) \varepsilon^2 \quad (12a)$$

where

$$\phi = \left(\frac{3\varepsilon}{10 + 6\varepsilon} \right)^{1/2}, \quad \varepsilon = \left(\frac{\rho_2}{\rho_1} - 1 \right) = f(M_1) \quad (12b)$$

with the density ratio across the shock expressed by the Rankine-Hugoniot relation for a normal shock.

Fig. 7 shows a comparison of the scattered sound intensity (in SPL) between Ribner's result (Ribner¹⁹) and that of Lighthill¹³, as presented by Ribner¹⁹. Significant discrepancy is noted between the two results. A critical discussion of this comparison is provided by Ribner¹⁹. (mention the scale for Ribner's and Lighthill's results)

2. Nonlinear Euler Simulations

Since the shock weakens as the Mach number tends to unity, the shock front will undergo greater distortions from an incident wave of fixed amplitude. Thus, nonlinear effects ought to be increasingly important for lower Mach numbers (Zhang et al.²⁹). Zhang et al.²⁹ validated the linear analysis of McKenzie and Westphal³³ by comparisons with their numerical solution of nonlinear 2D Euler equations. Although restricted in terms of the incident angle of the disturbance, it was shown that the linear analysis was valid over a surprisingly large range of shock strengths and disturbance amplitudes (Fig. 8). The comparisons suggest that the linear theory is fairly accurate for a wide range of incident angles up to the critical angle. Although comparisons were made for both the incident and the vorticity waves, only the comparisons for the incident vorticity waves are indicated in Fig. 8.

3. DNS Simulations

The simplest circumstance in which turbulence interacts with a shock wave is the case of isotropic turbulence interacting with a normal shock (transverse vorticity amplification). Lee et al.³⁵ performed DNS simulation of the interaction of 3-D isotropic turbulence ($0.06 \leq M_t \leq 0.11$) where M_t is the fluctuation Mach number (i.e., rms velocity/mean speed of sound upstream of the shock wave) with a normal shock ($1.05 \leq M_1 \leq 1.2$) where M_1 is the mean upstream Mach number. Detailed comparisons of DNS results to Ribner's linear analysis^{15,20} were made. Amplification (of turbulence) is more pronounced at the large wave numbers, which is consistent with the linear analyses. The turbulent kinetic energy is amplified across the shock wave, but this amplification tends to saturate beyond $M = 3$. DNS results for the amplification of kinetic energy of turbulence across a normal shock wave vs. linear theory is good. The rapid variation of k immediately behind the shock is connected with the decay of the acoustic energy in this region. The unsteady motion of the shock wave is found to reduce the amplification of the turbulent kinetic energy.

Subsequently stronger shock strengths ($M_1=2, 3$; $M_t=0.11$) were studied (Lee et al. 1997). DNS calculations by Lee et al.³⁶ agree with Ribner's theory for the measure of anisotropy downstream of the shock as $u'_2/v'_2=0.87$ at $M=3$ in agreement with Ribner's theory. The DNS studies also suggest that the isotropic turbulence becomes axisymmetric downstream of the shock. Numerical simulations by Rotman³⁷ and DNS calculations by Lee et al.^{34,35} show that the vorticity amplification predictions are in good agreement with the linear theory.

Fig. 9 shows a comparison of amplification of turbulent kinetic energy (k_2/k_1) in shock-turbulence interaction, as predicted by linear theory and DNS (Mahesh et al.³⁸, Lee et al.³⁶). This figure is adapted from Sinha et al.³⁹). Excellent agreement is noticed between the two computations up to $M_1 = 3$, beyond which the linear theory suggests an asymptotic trend in the amplification.

Although DNS solutions provide the most accurate representation of the shock/turbulence interaction, they seem to be impractical for conditions involving strong shock waves and high Reynolds number turbulence on account of resolution requirements of shock waves and turbulence.

B. Experimental Data

Experimental data suggest that in general compression enhances turbulence and expansion suppresses it. Measurements by Barre et al.⁴⁰ at $M_1 = 3$ suggest that the shock wave increases the longitudinal fluctuating velocity in agreement with Ribner's theory (Ribner¹⁹). As indicated by Ribner⁴¹, the measured amplification ratio of mean square longitudinal component of turbulence velocity (u_2^2/u_1^2) is close to the theoretical value of about 1.5 as predicted by Ribner's theory^{14,15} at $M_1 = 3$ (Fig. 10a)..

With regard to the anisotropy of turbulence downstream of the shock, the DNS calculations of Lee et al.^{34,35} and the linear theory of Ribner¹⁵ suggest that the anisotropy downstream of the shock $u'_2 / v'_2 = 0.87$ at $M_1 = 3$. This result considerably deviates from the measured value of 1.5 (Baïre et al.⁴⁰), as seen in Fig. 10b. Linear theory predicts a value of u'_2 / u'_1 in excess of unity only for upstream Mach numbers below 2, with the highest value shown to be about 1.1 (at $M_1 = 1.25$). As indicated by Ribner⁴¹, this discrepancy between the theory and the experiment remains puzzling.

IV PROPOSED THEORY

The discrepancy between the theories of Lighthill¹³ and of Ribner¹⁴ in comparison with the experimental data for the scaling of shock noise intensity (as evident from Fig. 7) requires further investigation. This discrepancy is attributed to the fact that in their theories the turbulence is treated effectively as a frozen spatial pattern without regard to the temporal fluctuations. There is thus a deficiency in applying linear theory to real turbulence, which consists of transient phenomena and not steady plane waves (Zhang et al.²⁹). Also, three-dimensional simulation is needed to accommodate vortex stretching (Zhang et al.²⁹).

The irregularity and disorderliness characterizing turbulence involve the impermanence of the various frequencies and of the various periodicities and scale (Hinze⁴²). In view of these circumstances these circumstances it is plausible that the peak angle of incidence is representative of the shock-shear wave interaction insofar as the scaling of the BBSN is concerned. Accordingly it is postulated here that the generation of sound at the peak incidence governs the generation of sound. Also it is assumed that the interaction of turbulence with the leading shock cell forms the maximum contribution to the intensity sound, and that the sound contribution due to the interactions at the subsequent shock cells is of secondary nature (subsidiary importance).

With the above postulate, the linear acoustic response (acoustic pressure rise) for shock-vortex interaction (vorticity waves incident on a shock) is shown in Fig. 12 for various upstream Mach numbers, as given by Ribner's theory (Ribner^{14,15}). The results point out that the peak angle of incidence and the associated acoustic response varies with the Mach number.

IV. RESULTS AND DISCUSSION

Based on the foregoing premise, the intensity of BBSN taken at the peak incidence angle is plotted as function of β (Fig. 10). This result reveals that the scaling of intensity very nearly varies as β^4 for a range of β between 0.2 and 2.0. In this range the present theory yields

$$I \propto \beta^{4.2} \quad (13)$$

Beyond this range there is seen a change in slope in the intensity variation.

A direct comparison of the scaling based on the proposed theory and the experimental data of Tanna²⁰ is presented in Fig. 13. The theory substantially agrees with the data in the range of $0.3 < \beta < 1.0$. It is known that beyond about $\beta = 1$, a Mach disc is formed, which alters the shock-cell structure. The large central portion of subsonic flow that develops downstream of the Mach disc considerably diminishes the noise generation.

The satisfactory explanation of the β^4 scaling law by the proposed theory suggests that the hypothesis of peak incidence angle for the generation of sound by shock-vorticity interaction is plausible. This forms an important contribution of the present work.

The determination of the directionality effects and spectral distribution of the BBSN are outside the scope of the present investigation, which is mainly concerned with the scaling law for broadband shock noise intensity. The fact

that only a single shock-cell/vortex interaction is considered here indicates that the shock noise intensity obtained by the present formulation is essentially omnidirectional.

V. CONCLUSION

A theory is proposed for the scaling of the broadband shock-associated noise in supersonic jets considering linear interaction between the shock wave and the vorticity wave on the basis of peak incidence angle for the turbulence. The hypothesis that the generation of sound at peak incidence angle is important is shown to satisfactorily describe the experimental scaling law for the broadband shock-associated noise intensity.

References

- ¹Lighthill, M.J., On sound generated aerodynamically, I. General theory, Proceedings of the Royal Society of London A, Vol. 211, No. 1107, 1952, pp. 564-587.
- ²Lighthill, M.J., On sound generated aerodynamically, II. Turbulence as a source of sound; Proceedings of the Royal Society of London A, Vol. 222, No. 1148, 1954, pp. 1-32.
- ³Ffowcs-Williams, J.E., The noise from turbulence convected at high speed, Proceedings of the Royal Society of London A, Vol. 255, No. 1061, 1963, pp. 469-503.
- ⁴Seiner, J.M., Advances in high speed jet aeroacoustics, AIAA paper 84-2275, 1984...
- ⁵Harper-Bourne, M., and Fisher, M.J., The noise from shock waves in supersonic jets, Noise Mechanisms, AGARD CP-131, paper 11, March 1973.
- ⁶Powell, A., On the mechanism of choked jet noise, Proceedings of the Physical Society of London B, Vol. 66, 1953a, pp. 1039-1056.
- ⁷Powell, A., The noise of choked jets, Journal of the Acoustical Society of America, Vol. 25, No. 3, 1953b, pp. 385-389.
- ⁸Kandula, M., Shock refracted acoustic wave model for screech amplitude in supersonic jets, AIAA J., Vol. 46, No. 3, pp. 682-689.
- ⁹Emden, R., Annln. Phy. Chem. 69, p. 426, 1899. (title)
- ¹⁰Prandtl, L., Phys. Z. Vol. 5, pp. 599-601, 1904. (title)
- ¹¹Rayleigh, Lord, Phil. Mag., Series 6, Vol. 32, 1916, pp. 177-181 (title).
- ¹²Pack, D.C., A note on Prandtl's formula for the wavelength of a supersonic gas jet, Q. J. Mech. Appl. Math., 3, pp. 173-181, 1950.
- ¹³Lighthill, M.J., On the energy scattered from the interaction of turbulence with sound or shock waves, Proc. Camb. Phil. Soc. 49, 1953, pp. 531-51.
- ¹⁴Ribner, H.S., Convection of a pattern of vorticity through a shock wave, NACA Report 1164, 1954 (supersedes NACA TN-2864, 1953).
- ¹⁵Ribner, H.S., Shock-turbulence interaction and the generation of noise, NACA Report 1233, 1955 (supersedes NACA TN-3255, July 1954).
- ¹⁶Fisher, M.J., Lush, P.A., and Harper-Bourne, M., Jet noise, J. Sound and Vibration, Vol. 28 (3), pp. 563-585, 1973.
- ¹⁷Howe, M.S., and Ffowcs Williams, J.E., On the noise generated by an imperfectly expanded supersonic jet, Philosophical Transactions of the Royal Society, Vol. 289, No. 1358, pp. 271-314, May 1978.
- ¹⁸Krothapalli, A., Soderman, P.T., Allen, C.S., Hayes, J.A., and Jaeger, S.M., Flight effects on the far-field noise of a heated supersonic jet, AIAA Journal, Vol. 35, No. 6, pp. 952-957, 1997.
- ¹⁹Ribner, H.S., Acoustic energy flux from shock-turbulence interaction, J. Fluid Mech., Vol. 35, part 2, 1969, pp. 299-310.

- ²⁰Ribner, H.S., Spectra of noise and amplified turbulence emanating from shock-turbulence interaction, *AIAA J.*, Vol. 25, 1987, p.p. 436-442.
- ²¹Tanna, H.K., An experimental study of jet noise, Part II: Shock Associated Noise, *Journal of Sound and Vibration*, Vol. 50, No. 3, pp. 429-444, 1977.
- ²²Seiner, J.M., and Norum, T.D., Experiments of shock-Associated Noise in Supersonic jets, *AIAA-79-1526.*, 1979.
- ²³Norum, T.D., and Seiner, J.M., Broadband shock noise from supersonic jets, *AIAA Journal*, Vol. 20, No. 1, pp. 68-73, 1982.
- ²⁴Pao, S.P., and Seiner, J.M., Shock-Associated noise in supersonic jets, *AIAA Journal*, Vol. 21, No. 5, pp. 687-693, 1983.
- ²⁵Tam, C.K.W., and Tanna, H., Shock-associated noise of supersonic jets from convergent-divergent nozzles, *J. Sound and Vibration*, Vol. 81, No. 3, 1982, pp. 337-358.
- ²⁶Tam, C.K.W., Stochastic model theory of broadband shock associated noise from supersonic jets, *J. Sound and Vibration*, Vol. 116, No. 2, 1987, pp. 265-302.
- ²⁷Tam, C.K.W., Broadband shock-associated noise of moderately imperfectly expanded supersonic jets, *Journal of Sound and Vibration*, Vol. 140, No. 1, 1990, pp. 55-71.
- ²⁸Kovaszny, L.S.G., Turbulence in supersonic flow, *Journal of Aerospace Sciences*, Vol. 20, No. 10, Oct. 1953, pp. 657-674., 682.
- ²⁹Zang, T.A., Hussain, M.Y., and Bushnell, D.M., Numerical computation of turbulence amplification in shock-wave interactions, *AIAA J.*, Vol. 21, No. 1, Jan 1984, pp. 13-21.
- ³⁰Blokhintzev, D.I., A moving sound pickup, *Doklady Akademii Nauk SSSR (Soviet Physics-Doklady)*, Vol. 47, 1945, pp. 22-25 (Also English Translation in *NACA* report).
- ³¹Burgers, J.M., On the transmission of sound waves through a shock wave, *Proceedings of the Koninklijke Nederlandse van Wetenschappen*, Vol. 49, 1946, pp. 273-281.
- ³²Moore, F.K., Unsteady oblique interaction of a shock wave with a plane disturbance, *NACA 1165, 1964 (NACA TN 2879, 1953?)*.
- ³³McKenzie, J.F., and Westphal, K.O., Interaction of linear waves with oblique shock waves, *Phys. Fluids*, Vol. 11, 1968, pp. 2350- 2362.
- ³⁴Batchelor, G.K., *The Theory of Homogeneous Turbulence*, Cambridge University Press, Cambridge, 1953.
- ³⁵Lee, S., Lele, S., and Moin, S.K., Direct numerical simulation of isotropic turbulence interacting with a weak shock wave, *Journal of Fluid Mechanics*, 1993, Vol. 251, pp. 533-562.
- ³⁶Lee, S., Lele, S.K., and Moin, P., Interaction of isotropic turbulence with shock waves: effect of shock strength, *Journal of Fluid Mechanics*, Vol. 340, p. 22, 1997.
- ³⁷Rotman, Shock wave effects on a turbulent flow, *Phy. Fluids*, Vol. 3, pp. 1792-1806, 1991.
- ³⁸Mahesh, K., Lele, S.K., and Moin, P., The influence of entropy fluctuations on the interaction of turbulence with a shock wave, *Journal of Fluid Mechanics*, Vol. 334, 1997, p. 353.

³⁹Sinha, k., Mahesh, K., and Candler, G.V., Modeling shock unsteadiness in shock/turbulence interaction, AIAA_2003-1265.

⁴⁰Barre, S., Allem, D., and Bonnet, J.P., Experimental study of a normal shock/homogeneous turbulence interaction, AIAA J., Vol. 34, No. 5, May 1996, pp. 968-974.

⁴¹Ribner, H.S., Comment on "Experimental study of a normal shock/homogeneous turbulence interaction, AIAA J., Vol. 36, No. 2., March 1998, p. 494.

⁴²Hinze, J.O., Turbulence, 2nd ed. McGraw-Hill, New York, 1975.

Kandula, M., On the scaling laws and similarity spectra for jet noise in subsonic and supersonic flow, Int. J. Acoustics and Vibration, Vol. 13, No. 1, pp. 3-16, March 2008.

Kandula, M., Near-field acoustics of clustered rocket engines, Journal of Sound and Vibration, Vol. 309, pp. 852-857, 2008.

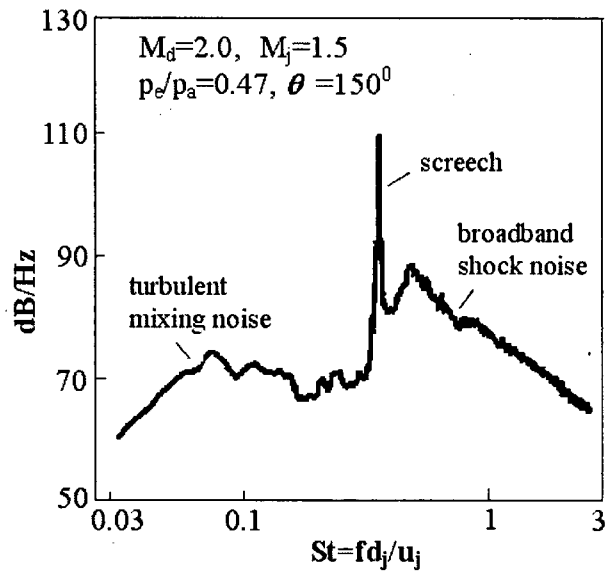


Fig. 1 A typical narrowband farfield shock noise spectrum (adapted from Seiner⁴).

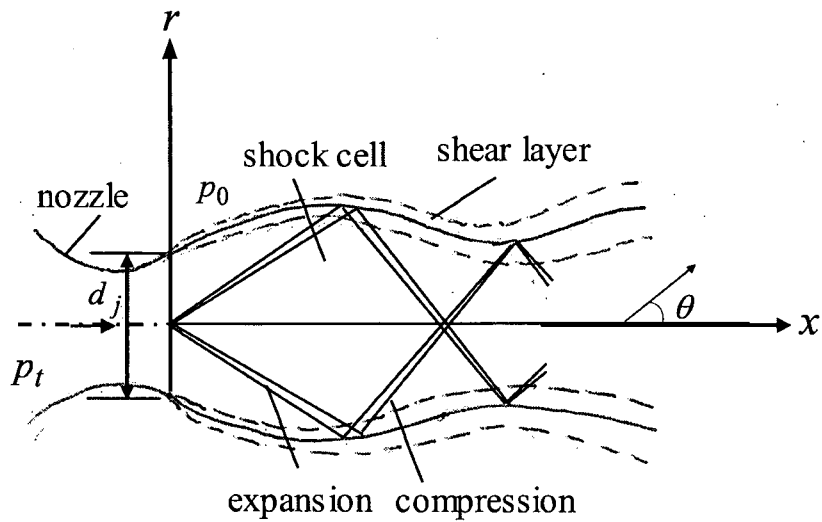


Fig. 2 Shock cell structure in imperfectly expanded supersonic jets.

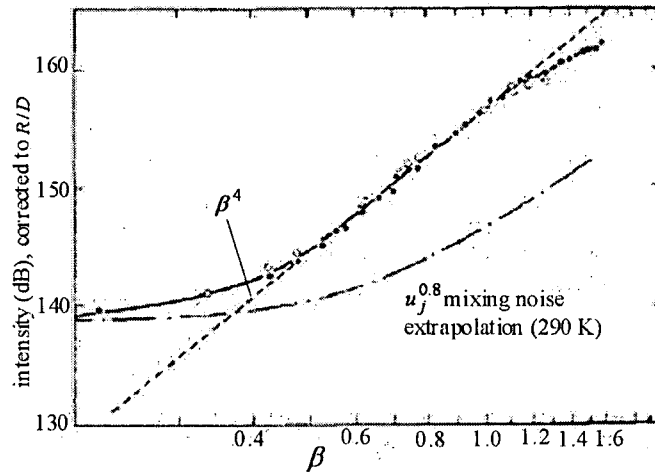


Fig. 3 Intensity of broadband noise at 90 deg. to jet axis (from Fisher et al.¹⁶)

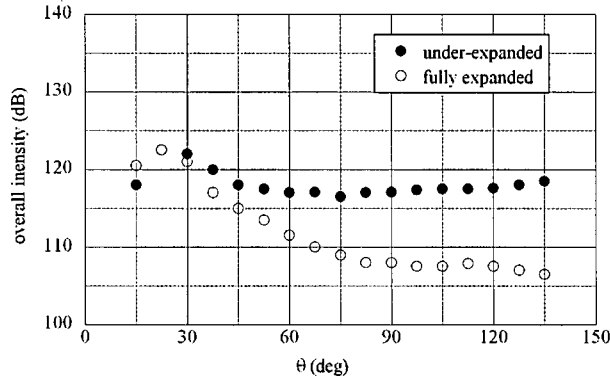


Fig. 4a Directivity of broadband shock noise (from Tanna²¹) at $\beta = 0.94$ and $T_j/T_0 = 0.73$.

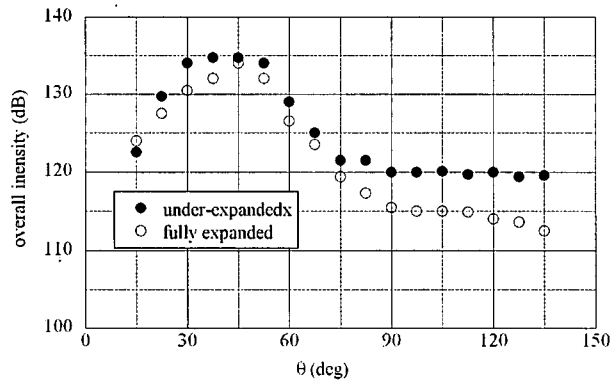


Fig. 4b Directivity of broadband shock noise (from Tanna²¹) at $\beta = 0.94$ and $T_j/T_0 = 2.272$.

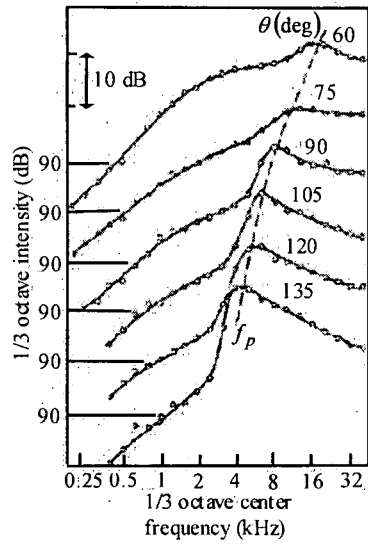


Fig. 5 Spectral character of broadband shock noise (from Tanna²¹).

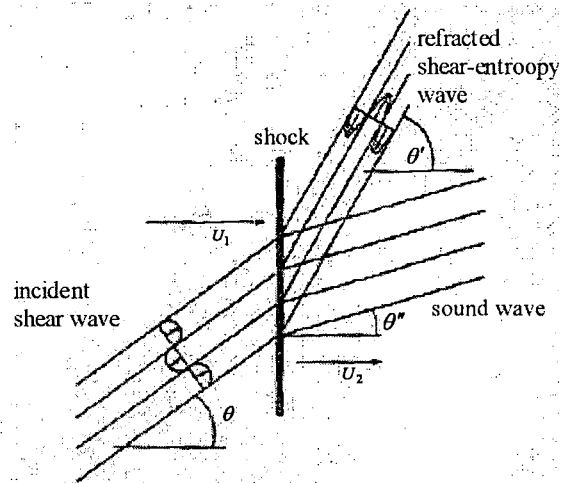


Fig. 6 Interaction of a shear wave with shock wave (Ribner¹⁹).

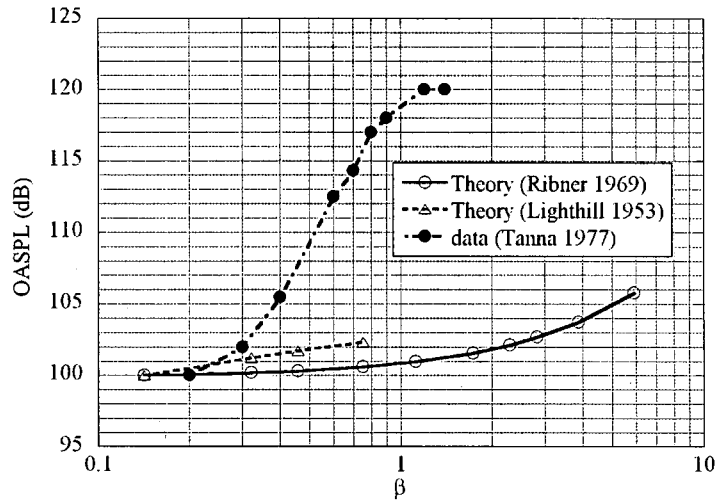


Fig. 7 Intensity of broadband noise according to the theories of Ribner¹⁹ and Lighthill¹³.

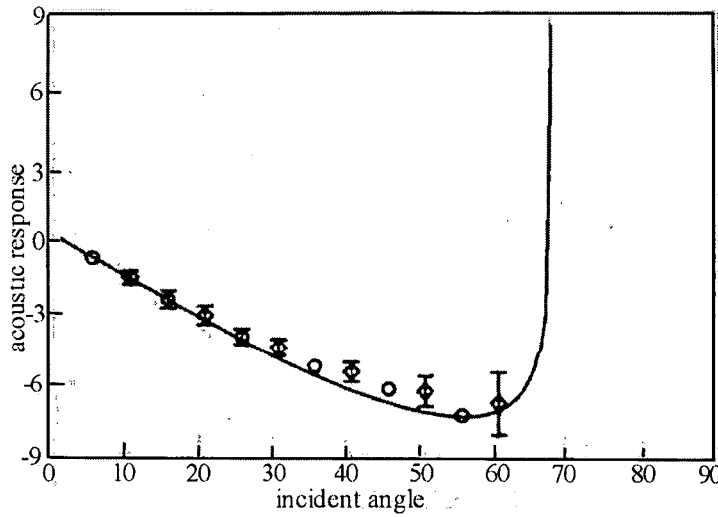


Fig.8 Dependence of acoustic response to vorticity waves incident on a Mach 8 shock (solid lines: linear theory, circles from nonlinear Euler simulations; from Zhang et al²⁹).

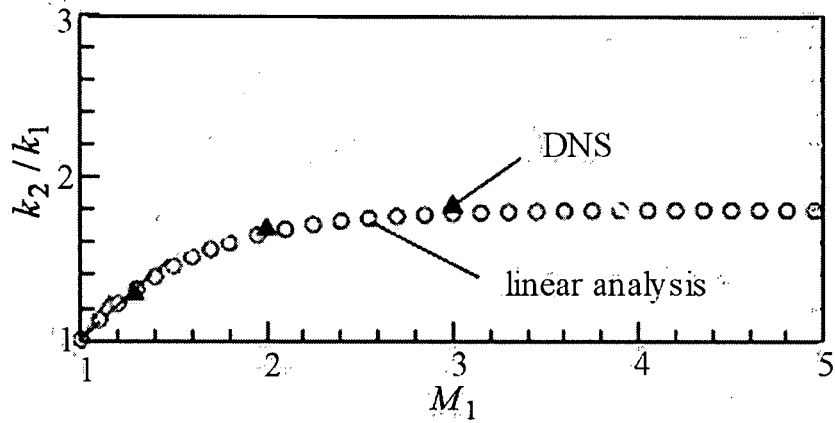


Fig. 9 Amplification of turbulence kinetic energy in shock-turbulence interaction, as obtained by linear theory and DNS (Mahesh et al.³⁷)

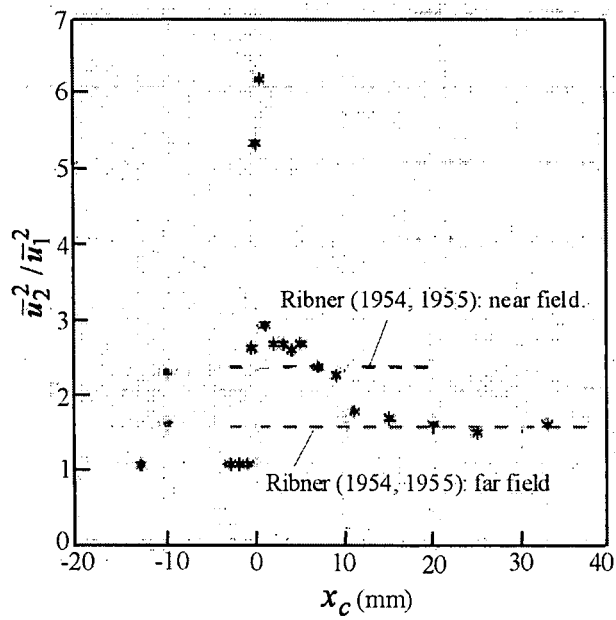


Fig. 10a Measured amplification of longitudinal velocity fluctuation across a shock in shock-turbulence interaction (Barre et al.⁴⁰).

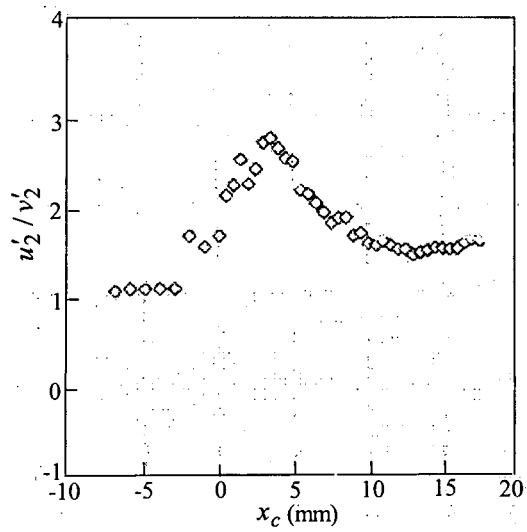


Fig. 10b Measured evolution of anisotropy across a shock in shock-turbulence interaction (Barre et al.⁴⁰).

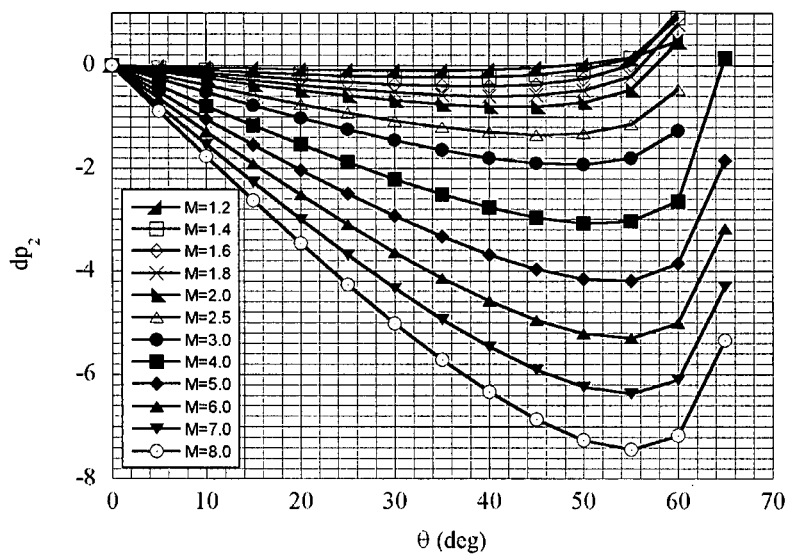


Fig. 11 Pressure rise due to shock/vorticity amplification (according to linear theory (Ribner¹⁴))

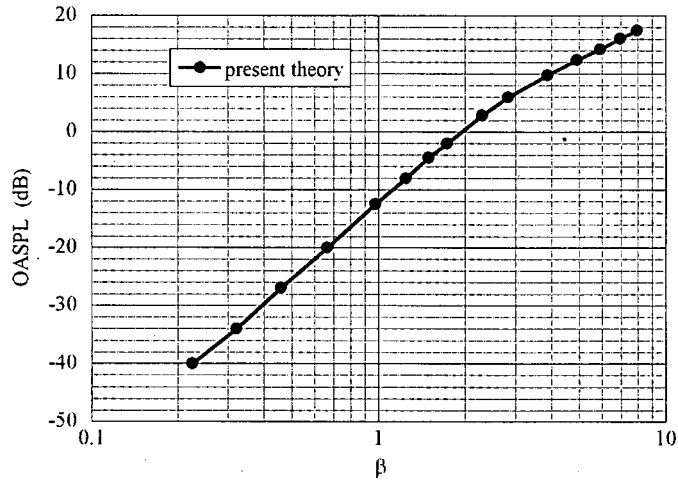


Fig. 12 Intensity of broadband noise according to the theory of maximum incidence angle.

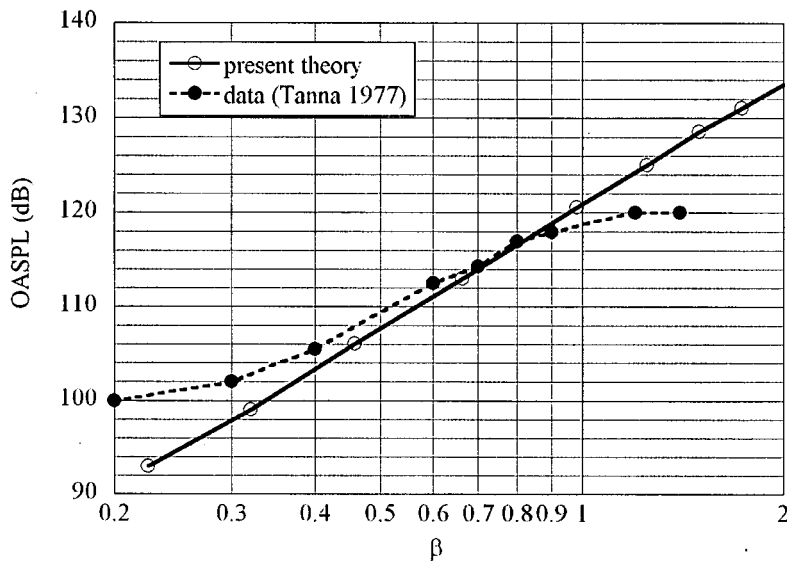


Fig.13 Comparison of the present theory and the data of Tanna²¹ for the intensity of the broadband shock noise.